Wind Energ. Sci. Discuss., https://doi.org/10.5194/wes-2019-22
Manuscript under review for journal Wind Energ. Sci.
Discussion started: 14 May 2019

eawe european academy of wind energy
Open Access WIND ENERGY SCIENCE DISCUSSIONS

The effect of wind direction shear on turbine performance in a wind farm in central Iowa

Miguel Sanchez Gomez[1], Julie K. Lundquist[2,3]

[1]Department of Mechanical Engineering, University of Colorado Boulder, Boulder, 80303, United States
[2]Department of Atmospheric and Oceanic Sciences, University of Colorado Boulder, Boulder, 80303, United States
[3]National Renewable Energy Laboratory, Golden, 80401, United States

Correspondence to: Miguel Sanchez Gomez (misa5952@colorado.edu)

Abstract. Numerous studies have shown that atmospheric conditions affect wind turbine performance, however, some findings have exposed conflicting results for different locations and diverse analysis methodologies. In this study, we explore how the change in wind direction with height (direction wind shear), a site-differing factor between conflicting studies, affects wind turbine performance. We utilized lidar and turbine data collected from the 2013 Crop Wind Energy eXperiment (CWEX) project between June and September in a wind farm in north-central Iowa. Directional wind shear was found to follow a diurnal cycle and to monotonically decrease with increasing wind speeds. Using different thresholds to distinguish between high- and low-directional wind shear scenarios, we found that larger thresholds evidence statistically-significant effects on turbine power production for lower wind speeds. We further analyzed a threshold of 0.225 deg m^{-1} and found turbine underperformance in the order of 10% for wind speed regimes below 8 m s^{-1}. Considering a time period of ramping electricity demand (0530 – 0900 LT) exposed the fact that large direction shear occurs during this time and is undermining turbine performance by more than 10%. A predominance of clockwise direction shear (wind veering) cases compared to counterclockwise (wind backing) was also observed throughout the campaign. Moreover, large veering was found to have greater detrimental effects on turbine performance compared to small backing values. This study shows that changes in wind direction with height should be considered when analyzing turbine performance, however, future work on segregating speed and direction shear should be pursued to quantify the effects of only one factor on turbine power production.

1 Introduction

Wind power generation directly depends on wind speed. Additionally, power depends on atmospheric conditions like static stability, shear and turbulence (e.g. Bardal et al., 2015; van den Berg, 2008; Kaiser et al., 2007; Rareshide et al., 2009; St. Martin et al., 2016; Sumner and Masson, 2006; Vanderwende and Lundquist, 2012; Wagner et al., 2010; Walter et al., 2009; Wharton and Lundquist, 2012). Idealized theories state that the power extracted by a wind turbine is a function of the blade element's efficiency (i.e. turbine blade design) and the available power flux through the disk swept by the blades (Burton et al., 2001). However, atmospheric turbine operating conditions diverge from simplified ones used for turbine

Wind Energ. Sci. Discuss., https://doi.org/10.5194/wes-2019-22
Manuscript under review for journal Wind Energ. Sci.
Discussion started: 14 May 2019

design. Varying inflow speed and direction profiles, turbulence, transient conditions, and wake effects from upwind turbines alter power production.

Static stability in the lower planetary boundary layer is governed by temperature gradients that drive or suppress buoyancy (Stull, 1988). Three stability regimes are usually established; stable, neutral, and unstable conditions, corresponding to a stratified, equilibrated, and convective atmosphere, respectively. Several means of quantifying atmospheric stability have been employed in wind energy studies, including the dimensionless wind shear exponent (α), turbulence intensity, bulk Richardson number, and the Obukhov length. While some field measurements have provided insight into how stability affects power production, conflicting results have been reported in differing locations. At a wind farm identified only as "West Coast North America", Wharton and Lundquist (2012a,b) found an increase in wind turbine power production during stable atmospheric regimes. In contrast, at another site in the central plains of North America, the opposite effect occurred (Vanderwende and Lundquist, 2012). St. Martin et al. (2016) considered the effects of stability and turbulence at a test site near the Rocky Mountains in Colorado. They found stable conditions to enhance performance near rated speed, while undermining it for lower wind speeds. Their results regarding turbulence effects, however, agreed with theoretical findings by Kaiser et al. (2007) and with observations presented by Rareshide et al. (2009) that suggest a convective atmosphere decreases performance near rated wind speed and causes overperformance near cut-in wind speed.

Several factors could explain the difference in results between these stability regimes. First, the available data and thus the analysis method differs. Wharton and Lundquist (2012b) segregated power production regimes using wind shear exponents and turbulence intensity in a location with channelled flow. In contrast, Vanderwende and Lundquist (2012) employed the Richardson number and wind shear criteria to quantify local atmospheric stability on a wind farm that could experience directional wind shear. The conflicting results among studies suggest that either additional forcing mechanisms are present or that site-specific factors govern the effects on power production. One likely site-specific factor is the role of directional wind shear, which was not explicitly considered in the above studies but could differ between those sites.

Here we sought to resolve these conflicting results by quantifying the role of directional wind shear in turbine performance. Directional shear is the change of wind direction with height. In the meteorological community, "wind veering" is used to describe the clockwise turning of the geostrophic wind with height, while "wind backing" describes the counter-clockwise turning of the geostrophic wind with height (Holton and Hakim, 2013). Veering tends to be associated with warm air advection, while backing is associated with cold air advection. Both these terms are associated with deep layers in the atmosphere rather than relatively shallow layers of the atmospheric boundary layer (ABL). Within the boundary layer, veering tends to be more common in the Northern Hemisphere due to the direction of the Coriolis force and the resulting Ekman layer.

In a wind energy context, directional shear causes the incoming wind to be misaligned with the rotor axis over some heights of the rotor swept area (Bardal et al., 2015) as the turbine tends to orient itself into the direction of the wind at hub height. Both veering and backing generate a substantial variation of the horizontal wind speed component orthogonal to the turbine axis. Veering decreases the mean relative wind speed experienced by a clockwise-rotating blade, while backing

increases it (Wagner et al., 2010). In contrast, the opposite happens for the angle of attack. The angle of attack is larger for veering and smaller for backing (Wagner et al., 2010). Simulations by Wagner et al. (2010) also show that though backing increases both mean lift and drag over the blade, the resulting tangential force experienced by the rotor is reduced, while it is slightly augmented by veering. The increase in tangential force from wind veering results in a slight increase in power production, whilst wind backing slightly decreases power production.

The existing studies on the effects of atmospheric stability on power production differ in the role of directional wind shear. The Wharton and Lundquist (2012a,b) wind turbines, and St. Martin et al. (2016) testing site were surrounded by complex terrain that prevented the development of directional wind shear during stable conditions. In contrast, at the Vanderwende and Lundquist (2012) location, complex terrain did not prevent the occurrence of a changing wind direction with height.

Several methodologies have been employed for studying the effects of directional wind shear on turbine performance. Bardal et al. (2015) used measurements from a test site in the coastline of Norway without distinguishing between veering and backing. They found a small reduced power output below rated speeds for directional shear above 0.05 deg m^{-1}. Rareshide et al. (2009) found slight effects on turbine performance for large wind backing values using measurements from several sites across the Great Plains/Midwest region. Walter et al. (2009) characterized directional shear in Texas and Indiana, and used those findings to run blade-element simulations using the National Renewable Energy Laboratory (NREL) fatigue analysis structures and turbulence (FAST) model. Results from coupling power change simulations with observations evidenced potential power gains as large as 0.5% and losses as low as 3% when considering both speed and direction shear. Simulations by Wagner et al. (2010) employed a simplified model (HAWC2) finding slight increases in power production for veering and larger reductions from backing, for constant wind speed shear values.

In this present study, the effects of directional wind shear on power production were analyzed using data collected in the 2013 Crop-Wind Energy eXperiment (CWEX-13) field campaign of a 150 MW onshore wind farm. Section 0 provides an overview of the dataset utilized for this study, which includes turbine power production and wind profiling lidar, and their respective filtering. Section 0 describes the definition of directional wind shear and individual turbine's power curves. Directional shear characterization and its effects on turbine power production are outlined in sections 0 and 0.

2 Data

2.1 Measurement site

The Crop Wind Energy eXperiment projects (CWEX) in 2010, 2011 and 2013 intended to quantify how wind turbines create changes in microclimates over crops (Rajewski et al., 2013, 2014, 2016), how the diurnal cycle affects wind turbine wakes (Lee and Lundquist, 2017; Rhodes and Lundquist, 2013), and how agricultural cropping and surface management impact wind energy production (Vanderwende and Lundquist, 2016). The 2013 campaign emphasized the impacts of atmospheric conditions like nocturnal low-level jets (Vanderwende et al., 2015) on wind turbine performance and the

Wind Energ. Sci. Discuss., https://doi.org/10.5194/wes-2019-22
Manuscript under review for journal Wind Energ. Sci.
Discussion started: 14 May 2019

dynamics of wake variability (Bodini et al., 2017; Lundquist et al., 2014). The CWEX-13 field campaign took place between late June and early September 2013 in a wind farm in north-central Iowa. Measurements from several surface flux stations, a radiometer, three profiling lidars, and a scanning lidar were collected. These data have also been used to test approaches for coupling mesoscale and large-eddy simulation models (Muñoz-Esparza et al., 2017).

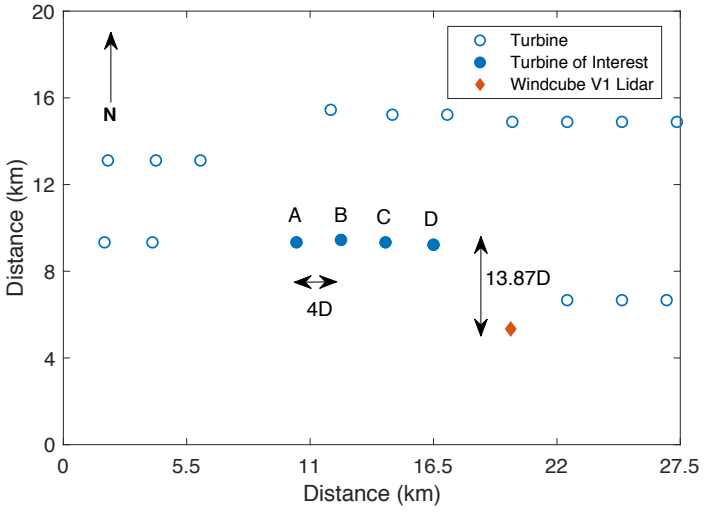

Figure 1. Schematic diagram of CWEX-13 region of interest.

The wind farm consists of 200 wind turbines extending in a parallelogram with a long axis from the southeast to northwest. The northernmost 100 turbines are General Electric (GE) 1.5 MW extra-long extended (XLE) model and the southernmost 100 turbines are GE 1.5 MW super-long extended (SLE) model turbines. The land is generally flat with a slope smaller than 0.5 deg from southwest to northeast. Turbines are surrounded by a mixture of corn and soybeans, some wetland and lower terrain at the southern edge of the farm, and scattered farmsteads (Rajewski et al., 2013). The region of interest in the 2013 campaign comprises a subset of GE 1.5 MW XLE model turbines (see Table 1 for specifications). For this study, power production from four turbines near one Windcube V1 profiling lidar was utilized (Figure 1).

Table 1. Technical specifications of the turbines studied in the CWEX-13 field campaign (General Electric, 2009)

Rotor diameter (D)	82.5 m
Hub height	80 m
Rated power	1.5 MW
Cut-in wind speed	3.5 m s^{-1}
Rated power at	11.5 m s^{-1}
Cut-out wind speed	20 m s^{-1}

Wind Energ. Sci. Discuss., https://doi.org/10.5194/wes-2019-22
Manuscript under review for journal Wind Energ. Sci.
Discussion started: 14 May 2019

eawe european academy of wind energy
Open Access WIND ENERGY SCIENCE DISCUSSIONS

2.2 Lidar

To quantify directional wind shear, we rely on data collected from the profiling lidar Windcube V1, designed by Leosphere, deployed during the CWEX-13 campaign. This Doppler wind lidar measures vertical profiles of speed and direction at nominally 1-Hz temporal resolution. It uses a Doppler beam swinging (DBS) approach obtaining radial wind measurements along four cardinal directions at an inclination of 62.5º above the horizon (Vanderwende et al., 2015). The components of the flow are then calculated from the four separate line-of-sight velocities (Lundquist et al., 2015). The CWEX-13 campaign collected wind measurements from 40 to 220 m above ground level at 20 m increments. This study focuses on 2-min average measurements from 40 to 120 m, which comprise the entire turbine rotor layer.

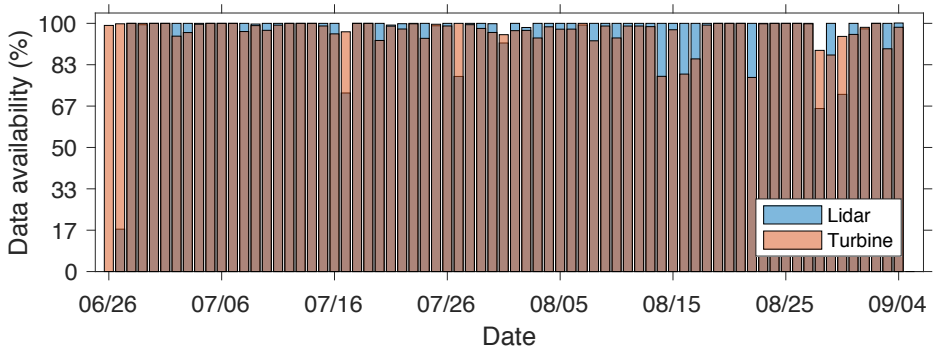

Figure 2. Lidar and turbine data availability for the duration of the campaign. Turbine power availability only corresponds to wind speeds above 2.5 m s^{-1}.

Wind lidar data is available throughout the campaign (Figure 2), only having significant shortages (>30% of day) for June 27 and August 28. Likewise, turbine power data availability for wind speeds above 2.5 m s^{-1} presented great uniformity, having largest shortages (>20%) for August 14, 16 and 22, and an average 30-min availability of 92%.

The prevailing wind direction for the recorded period in this wind plant was primarily south-southwesterly having a mean wind speed of 8.21 m s^{-1}. However, 21% of wind has a strong northerly component (Figure 3), generally associated with frontal passages. The infrequent easterly and westerly winds (90±10 deg and 270±10 deg) were discarded to ensure the turbines were not experiencing wakes from their nearby (within 5 rotor diameters D) neighbors. Previous studies in this wind farm have found wakes in stable conditions to persist for long distances (up to 17.5 D) downwind (Bodini et al., 2017), and so therefore all winds with northerly components were also discarded to ensure the profiling lidar was not affected by wakes. Further, only wind speeds between cut-in (3.5 m s^{-1}) and cut-out (20 m s^{-1}) were considered.

Wind Energ. Sci. Discuss., https://doi.org/10.5194/wes-2019-22
Manuscript under review for journal Wind Energ. Sci.
Discussion started: 14 May 2019

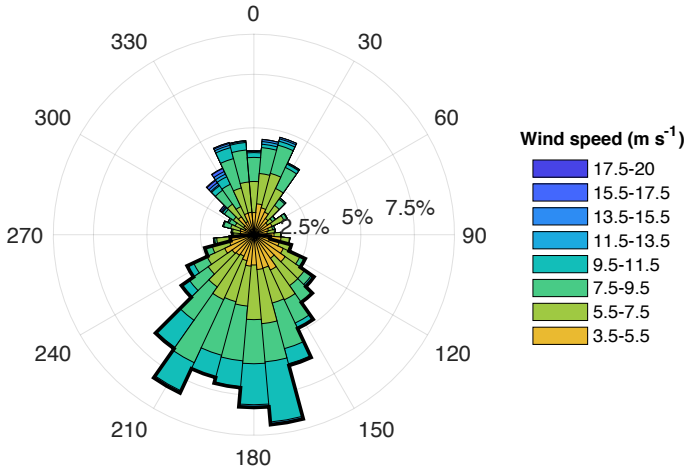

Figure 3. Wind rose for lidar hub-height altitude (80-m) measured wind speeds between cut-in and cut-out. The black outline highlights the wind direction sector (southerly) used for subsequent data analysis.

The remaining analysis only considers winds with southerly components (wind direction between 100 and 260 deg), and speeds between 3.5 and 20 m s^{-1}. Of note, most winds above 11 m s^{-1} occurred with the northerly frontal passages, so this direction filtering also effectively restricts the analysis to wind speeds below 11 m s^{-1}.

2.3 Wind turbines

The subset of turbines employed for this study consists of four GE XLE 1.5-MW, variable blade pitch wind turbines (see Table 1 for specifications). Power production, nacelle wind speed and blade pitch angles were provided by the wind farm operator as 10-min averages recorded via the supervisory control and data acquisition (SCADA) system of each turbine. To analyze how directional wind shear impacts power production, turbine underperformance during curtailments was filtered following the blade pitch angle approach of St. Martin et al. (2016). Blade pitch angles are controlled to maximize power production as a function of nacelle-measured wind speed, and large blade pitch angles typically represent curtailed conditions or rapidly changing conditions. Therefore, we discarded 10-min periods with blade pitch angles outside $\pm$4.5 the mean absolute deviation (MAD) for each 0.5 m s^{-1} wind speed bins (Figure 4).

Wind Energ. Sci. Discuss., https://doi.org/10.5194/wes-2019-22
Manuscript under review for journal Wind Energ. Sci.
Discussion started: 14 May 2019

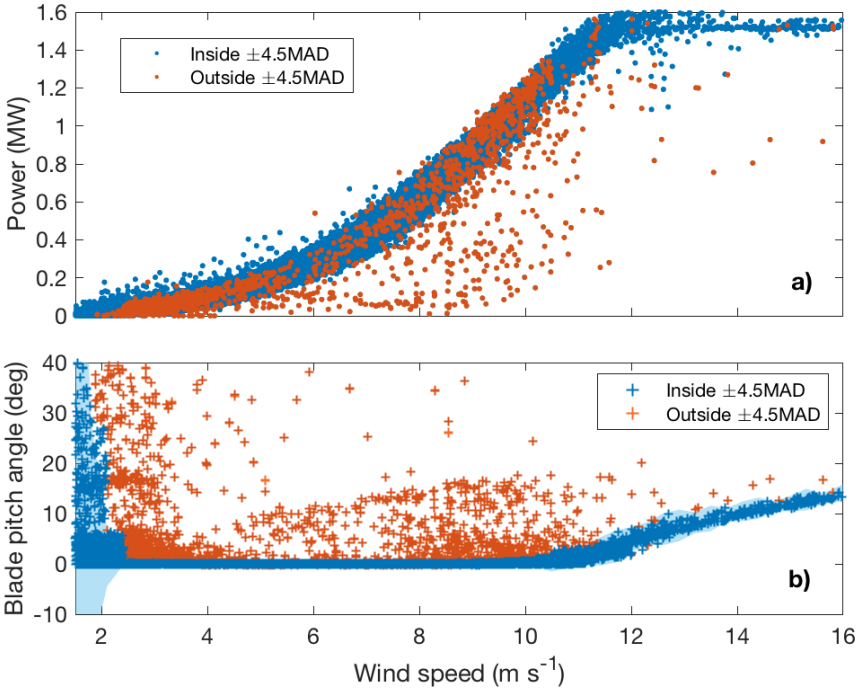

Figure 4. Power curve based on nacelle-measured wind speed (a), and blade pitch angle from a single blade (b). Red scatter points show 10-min periods filtered out for curtailments, represented by data points outside the MAD envelope. Blue envelope in bottom graph represents ±4.5 MAD of the blade pitch angle within 0.5 ms^{-1} wind speed bins.

2.4 Time averaging

Turbine- and lidar-recorded data are averaged over different time periods. Matching turbine performance with atmospheric conditions was performed by averaging lidar measurements for the corresponding 10-min-period.

3 Methods

3.1 Turbine power curves

According to the International Electrotechnical Commission's Wind Turbine Power Performance Standard (2005), wind turbine power performance characteristics are determined both by the measured power curve and the annual energy production. The measured power curve is obtained by simultaneously collecting data from meteorological variables and turbine performance over long periods of time. Wind speed is measured at hub height using cup anemometers mounted on a meteorological mast positioned 2 – 4 rotor diameters upwind of the turbine, and power output is recorded using a power measurement device (e.g. power transducer) between the wind turbine and the electrical connection. Measurements are averaged over 10-min time periods. A database for a wide range of wind speeds (0.5 m s^{-1} bins) is used to establish the

Wind Energ. Sci. Discuss., https://doi.org/10.5194/wes-2019-22
Manuscript under review for journal Wind Energ. Sci.
Discussion started: 14 May 2019

eawe european academy of wind energy
Open Access WIND ENERGY SCIENCE DISCUSSIONS

relationship between the nacelle-height wind speed and wind turbine power output. General Electric's power curve for the 1.5 MW wind turbines in this study is shown in Figure 5 as the dashed line.

Power production for the duration of this campaign reflected persistent differences from the manufacturer's reference values at wind speeds below 8 m s^{-1} and above rated (Figure 5). Consequently, mean power curves for each turbine were utilized as a reference value to have a consistent comparison of normalized performance among individual devices. Turbine power curves using nacelle-measured wind speed, and lidar-measured wind speed filtering easterly, westerly and northerly winds were compared. The Pearson correlation coefficient was used in each case to determine which power curve showed highest correspondence to the manufacturer's power curve for wind speeds below rated. Power curves obtained using lidar-measured wind speed displayed higher resemblance to GE curves (average $\rho = 0.9590, p = 0.00$) than power curves obtained from nacelle-measured wind speed (average $\rho = 0.9061, p = 0.00$). Therefore, normalization was performed with respect to each turbine mean power curve obtained using lidar-measured wind speed.

As suggested by the histogram in Figure 5, the frequency of occurrence changes with wind speed, roughly following a Weibull distribution with a shape factor of 4.1 and a scale factor or 8.2. To determine if the sample size (number of power observations) for each 0.5 m s^{-1} wind speed bin was large enough for estimating each turbine's population mean (observed power curve), we calculated the required sample size to have a 99% confidence that the error (e) in the observed mean power does not exceed half the difference of mean power between two adjacent wind speeds. The power estimator ($\hat{p}$) is assumed to be a normally distributed estimator of the real turbine power (p) for each wind speed bin, then their difference is a normal distribution (Walpole, 2007):

$$\frac{\hat{p}-p}{\sqrt{Var(\hat{p})}} \sim N(0,1)\ , \tag{1}$$

The allowable error was designated as half the difference in mean power between two adjacent wind speeds ($e_V = 0.5\,(\hat{p}_{V+0.5} - \hat{p}_V)$), and so the probability of the real and observed mean difference being greater than the allowable error ($P(|\hat{p}_V - p_V| > e_V)$) is 0.01 (i.e. 99% confidence). A property of a normal distribution is that this same probability holds for $|\hat{p}_V - p_V| > z_{\alpha/2}\,\sigma_V/\sqrt{n_V}$. Thus, the minimum sample size to have 99% confidence that the error in the observed mean power does not exceed half the difference of mean power between two adjacent wind speeds is $n_V = z_{\alpha/2}\,\sigma_V\sqrt{e_V}$. Every turbine had sufficient data points for wind speeds between 4 and 11 m s^{-1} (referred to as the partial load regime), and every 0.5 m s^{-1} bin within this range had at least 106 observations, supporting the assumption for a normally distributed estimator.

Wind Energ. Sci. Discuss., https://doi.org/10.5194/wes-2019-22
Manuscript under review for journal Wind Energ. Sci.
Discussion started: 14 May 2019

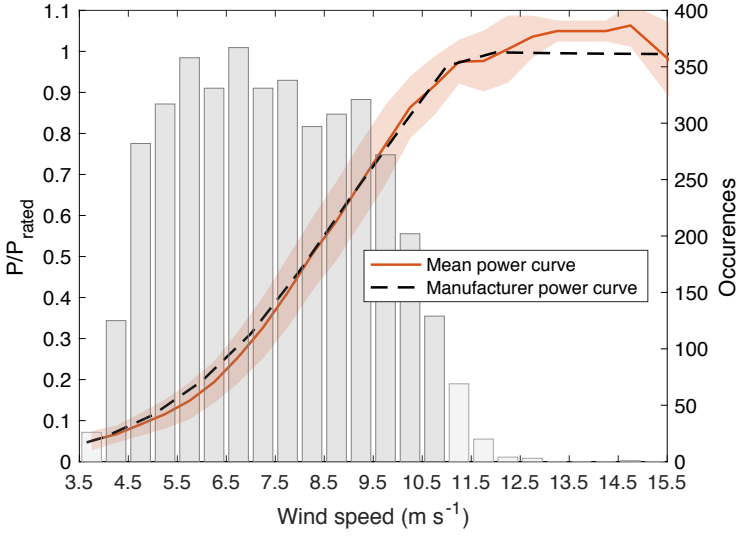

Figure 5. Mean power curve for Turbine C based on 80-m lidar wind speed measurements overlayed over the number of power production cases for each 0.5 m s^{-1} wind speed bins. The shaded region in the power curve corresponds to ±1 standard deviation, and the dark grey histogram corresponds to the wind speed ranges considered in this study.

Directional wind shear

Directional wind shear is defined as the change in wind direction with height. One mechanism for generating directional wind shear is the vertical shear of geostrophic wind referred to as thermal wind. The thermal wind is caused by large-scale horizontal temperature gradients that can be created by sloping terrain, fronts, land-sea interfaces, and large-weather patterns (Stull, 1988). Wind shear overnight is also generated by the inertial oscillation (Blackadar, 1957; Van de Wiel et al., 2010). The inertial oscillation is the rotation in the wind vector in the residual layer caused by a force imbalance at sunset, when mixed layer turbulence ceases. As frictional stress diminishes after sunset, pressure gradients tend to accelerate subgeostrophic winds in the mixed layer back toward geostrophic. Inertia from the counteracting Coriolis force induces an oscillation in the wind vector causing it to become supergeostrophic and to turn clockwise (northern hemisphere) with time (Stull, 1988). A third forcing mechanism is frictional drag with the ground. Turbulent momentum fluxes in the boundary layer reduce the actual wind speed near the surface. The Coriolis force, being directly proportional to the wind speed, decreases creating a force imbalance with the pressure gradients. As a result, the actual surface wind vector is directed across the isobars toward low pressure (Holton and Hakim, 2013).

Directional shear in this study is calculated as the absolute value of the shortest rotational path between wind vectors at 40 and 120 m above ground level, normalized over vertical distance between the measurements. For example, a case with southerly winds at 40 m and westerly winds at 120 m would be calculated as 90 deg shear over the 80 m layer depth, or 1.125 deg m^{-1}.

Wind Energ. Sci. Discuss., https://doi.org/10.5194/wes-2019-22
Manuscript under review for journal Wind Energ. Sci.
Discussion started: 14 May 2019

eawe european academy of wind energy
Open Access WIND ENERGY SCIENCE DISCUSSIONS

The literature includes a range of different classification thresholds to analyze contrast high directional wind shear (HDWS) and low directional wind shear (LDWS) to explore its effects on turbine performance. Bardal et al. (2015) utilized a threshold of 5 deg over a vertical extent of 100.6 m (or 0.0497 deg m^{-1}) to distinguish between HDWS and LDWS scenarios in a wind farm on the coastline of mid-Norway. They found small detrimental effects of HDWS on power production for wind speeds near 7, 8 and 9.5 m s^{-1} (Bardal et al., 2015). Rareshide et al. (2009) considered a statistical description specific to several sites across the Great Plains/Midwest region, encountering slight performance reductions for wind backing of 0.25 deg m^{-1}. Walter et al. (2009) performed blade-element modeling using the fatigue analysis structures and turbulence model (FAST) from the National Renewable Energy Laboratory to quantify the effects of speed and direction shear on performance. Simulation results for 8 and 10 m s^{-1} wind speeds showed a maximum instantaneous 6% underperformance occurring for wind shear exponents of 0.35 and wind backing of 0.472 deg m^{-1}. Here we considered different thresholds to define HDWS scenarios in order to identify power production differences compared to LDWS cases. HDWS scenarios for the 10-min power production periods where defined as those having the 10-min mean directional wind shear above the selected threshold, or having more 2-min HDWS than LDWS cases.

4 Results

4.1 Directional wind shear characterization

A predominance of wind veering was observed in this site compared to wind backing cases (Figure 6a). Wind veering occurred more than 77% of the time and displayed larger numerical mean and maximum values (0.0939 deg m^{-1} and 1.83 deg m^{-1}, respectively) compared to backing (-0.0144 deg m^{-1} and -1.17 deg m^{-1}, respectively). Figure 6b illustrates how wind direction evolves differently through the rotor layer for veering and backing cases. Both clockwise and counterclockwise wind direction rate of change is larger in the lower rotor layer. Directional shear is 1.6 times larger from 40 to 60 m compared to 100 to 120 m above ground level for veering, and 1.79 times larger for backing. When considering the absolute value of the wind vector rotation, the lower layer (40 to 60 m) experienced an average change in wind direction 1.55 times larger than the upper layer (100 to 120 m).

Wind Energ. Sci. Discuss., https://doi.org/10.5194/wes-2019-22
Manuscript under review for journal Wind Energ. Sci.
Discussion started: 14 May 2019

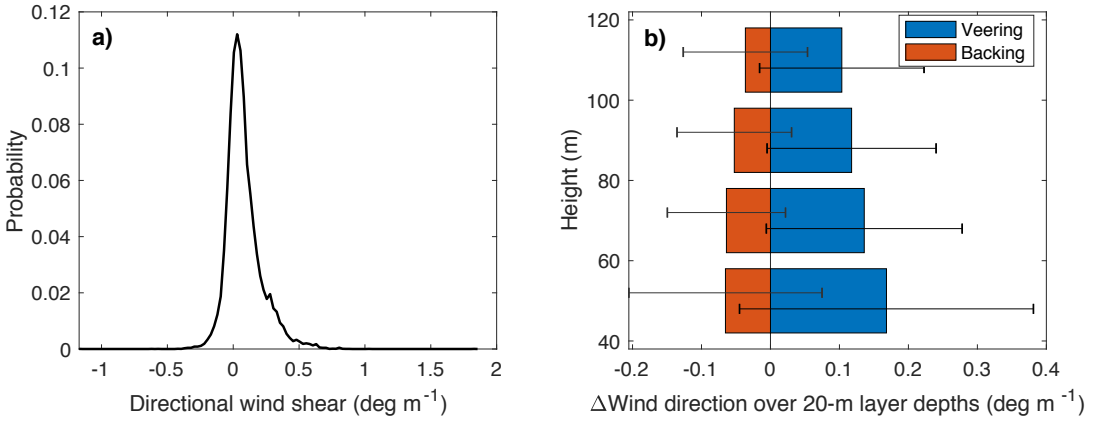

Figure 6. Probability distribution for direction shear (a), and wind direction evolution (b) in the rotor layer (40 – 120 m above ground level).

Directional wind shear at the test site varied with time of day (Figure 7). Nighttime cases showed an evolving surface layer that does not reach equilibrium, as is depicted by consistently increasing directional shear across the rotor layer at an average rate of 0.0304 deg m^{-1} hr^{-1} from before sunset until just after sunrise. Daytime cases, on the other hand, experienced a rapid morning transition following sunrise (-0.1171 deg m^{-1} of directional shear per hour) followed by a fairly consistent surface layer having a slowly decreasing mean directional shear of 0.004 deg m^{-1} per hour. Average changes in wind direction with height at night was 2.6 times larger than during daytime after the transition period.

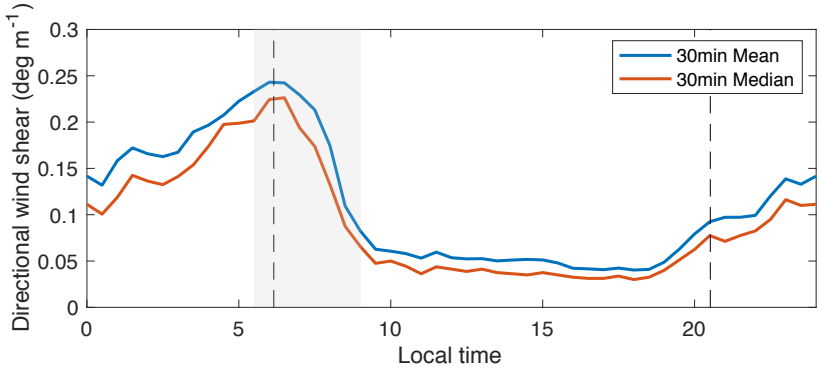

Figure 7. Diurnal cycle of directional wind shear for wind speeds between cut-in and cut-out. Dashed lines indicate sunrise and sunset times for August 1, 2013, the mid-point of the dataset analyzed here. The grey shaded region indicates the morning transition period (0530 – 0900 LT).

As directional shear varied throughout the day, it also had an inverse monotonical relationship with wind speed. Directional shear decreased with increasing wind speed for both daytime and nighttime cases (Figure 8). While directional shear at night was generally larger than during the day, in both cases direction shear decreased at a median rate of around 0.0166 deg m^{-1} for each increase in m s^{-1} in wind speed. Daytime is defined as the period between sunrise as sunset for each date, and nighttime corresponds to the complementary period. Daily sunrise and sunset information were estimated using

Wind Energ. Sci. Discuss., https://doi.org/10.5194/wes-2019-22
Manuscript under review for journal Wind Energ. Sci.
Discussion started: 14 May 2019

NOAA's sunrise/sunset calculator (National Oceanic and Atmospheric Administration, 2019). Median values appear in Figure 8 rather than mean values as the data presented a large spread with a large percentage of outliers. Outliers are considered observations outside the quantile 3 (75th percentile range) plus or minus a predetermined interquartile range (range between 25th and 75th percentile) for each 0.5 m s^{-1} wind speed bins (Q3±1.5IQ).

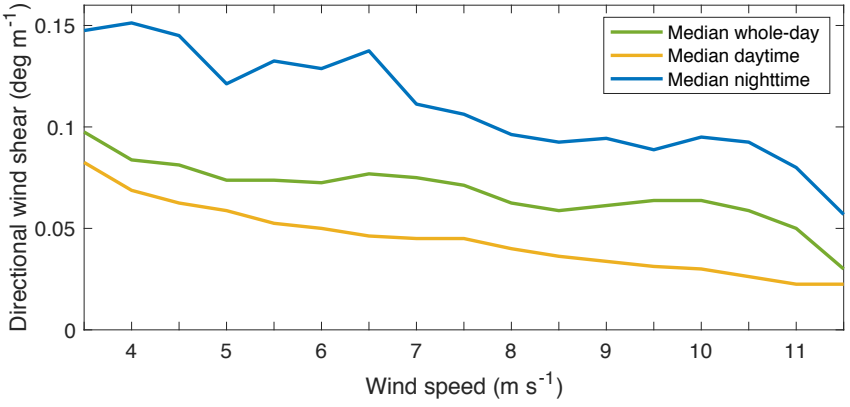

Figure 8. Directional wind shear variation with 80-m wind speed using each day's sunrise/sunset times of day.

Median nighttime directional wind shear was at least 1.8 times as large as daytime cases for wind speeds between cut-in and rated speed (Figure 8). The highest percentage difference occurs near rated wind speeds, where nighttime directional shear is 3.5 times larger than that during the day.

Of particular interest is the morning time period (from 0530 to 0900 local time) which, according to the U.S. Energy Information Administration (2019), experiences increasing electricity demand. Directional wind shear presented its largest rate of change during this time period (Figure 7). At this time, nearly 60% of the recorded data between cut-in and cut-out wind speed was within 4 and 8 m s^{-1} with a mean directional shear of 0.2257 deg m^{-1}. This average directional shear exceeds the mean daytime (0.0838 deg m^{-1}), whole-day (0.1137 deg m^{-1}), and nighttime (0.1613 deg m^{-1}) values.

Wind Energ. Sci. Discuss., https://doi.org/10.5194/wes-2019-22
Manuscript under review for journal Wind Energ. Sci.
Discussion started: 14 May 2019

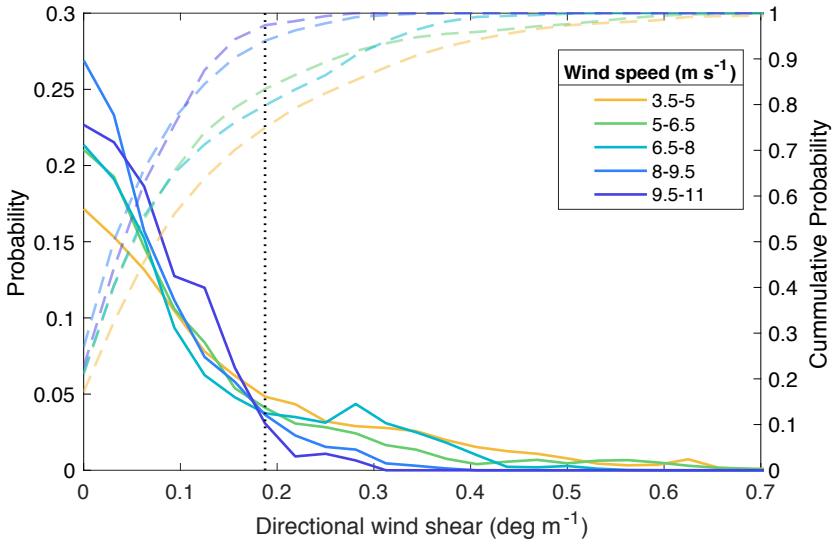

Figure 9. Directional wind shear probability density (solid lines) and cummulative (dashed lines) distributions for 1.5 m s^{-1} wind speed regimes. The black dotted line marks 0.1875 deg m^{-1} of directional wind shear.

The number of occurrences of directional wind shear cases above 0.1875 deg m^{-1} in this site varied considerably for wind speeds above and below 8 m s^{-1} (Figure 9). The number of observed cases of directional shear larger than 0.1875 deg m^{-1} follows a similar trend for wind speeds between cut-in and 8 m s^{-1}, accounting for approximately 80% of observations. Conversely, wind speeds between 8 m s^{-1} and rated speed report considerably fewer cases above 0.1875 deg m^{-1} of directional shear (~4% of observations for each 1.5 m s^{-1} wind speed bin).

4.2 Effects on turbine performance

Because one of the main differences between the Wharton and Lundquist (2012b) and Vanderwende and Lundquist (2012) studies was the occurrence of directional wind shear at the different sites, we here examined the effect of the shear of wind direction on turbine performance. We tested a range of threshold values of directional shear to distinguish HDWS and LDWS scenarios. Figure 10 illustrates the normalized difference in power output between high- and low-shear scenarios defined by different thresholds for different wind speed regimes.

Wind Energ. Sci. Discuss., https://doi.org/10.5194/wes-2019-22
Manuscript under review for journal Wind Energ. Sci.
Discussion started: 14 May 2019

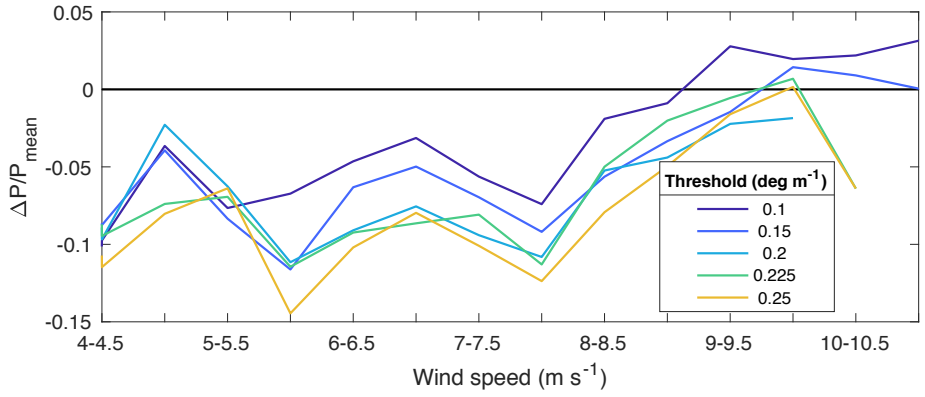

Figure 10. Mean normalized power production differences for high and low directional wind shear scenarios defined using different thresholds based on lidar 80-m height wind speed.

As larger HDWS thresholds were considered, the effect on power production starts to be reflected at lower wind speeds (Figure 10). Thresholds below 0.1 deg m^{-1} failed to distinguish power production in a statistically-significant way (the detailed significance estimates for specific wind speeds and turbines are not shown). Using a threshold of 0.1 deg m^{-1}, none of the four individual turbines agreed on a 0.5 m s^{-1} wind speed regime in which they had different medians with 5% significance for high and low directional shear cases. Individual turbines only agreed in mean normalized power production differences with 95% confidence for wind speeds between 7.5 and 8 m s^{-1}. A 0.15 deg m^{-1} directional shear limit only resulted in one 0.5 m s^{-1} wind speed range (7.5 – 8 m s^{-1}) where individual turbines agreed in both the median and mean differences (95% confidence) of normalized power production. Considering a threshold of 0.2 deg m^{-1} exposed more dissimilarities between high and low directional wind shear scenarios. Mean and median differences for individual turbines and their combined normalized power production matched for wind speeds between 7 and 8 m s^{-1} (5% significance for individual turbines, and 1% significance when combining the four turbines). Increasing the threshold to 0.225 deg m^{-1} also incorporated significant differences for all individual turbines in normalized power production for wind speeds between 6.5 and 7 m s^{-1}, resulting in a 1.5 m s^{-1} range of wind speeds (6.5 – 8 m s^{-1}) with observed power reductions for HDWS scenarios. Considering a threshold of 0.25 deg m^{-1} revealed turbine underperformance for an even lower wind speed range (5.5 – 6 m s^{-1}), however one turbine failed to have significant (95% confidence) mean normalized power reductions for wind speeds between (6.5 – 7 m s^{-1}).

Wind Energ. Sci. Discuss., https://doi.org/10.5194/wes-2019-22
Manuscript under review for journal Wind Energ. Sci.
Discussion started: 14 May 2019

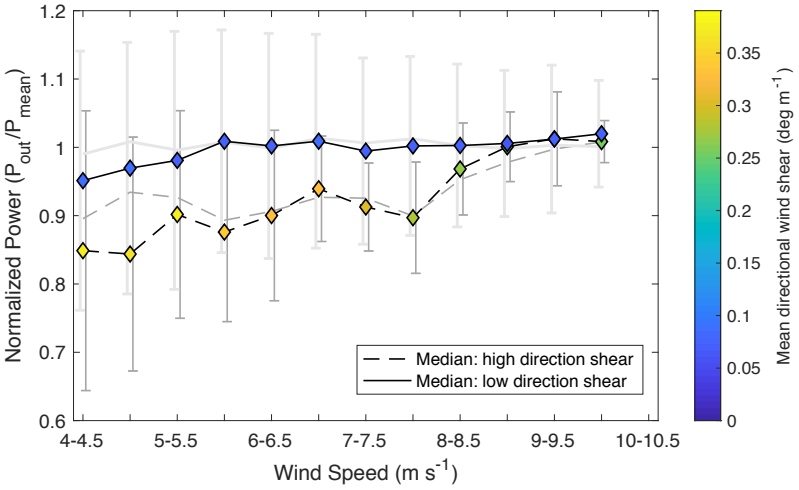

Figure 11. Normalized power production for high and low directional wind shear scenarios defined using a threshold of 0.225 deg m^{-1}. Black lines correspond to median values and grey ones to mean values. Error bars represent 1 absolute deviation from the median. Only 0.5 m s^{-1} wind speed bins with more than 30 data points are plotted.

For a threshold of 0.225 deg m^{-1}, the effects of HDWS on combined-turbine power production were most significant for wind speeds below 8 m s^{-1} (Figure 11). Combined mean normalized power was significantly (99% confidence) affected by HDWS for 4 – 4.5 and 5 – 8 m s^{-1} wind speed regimes. Mean turbine performance was in average 9.3% lower (1.64% standard deviation) for HDWS scenarios compared to LDWS cases for the formerly mentioned wind speed regimes. Combined median normalized power revealed significantly affected (5% significance) performance for HDWS scenarios for 4 – 8 m s^{-1}. Median underperformance was in the order of 10% (2.2% standard deviation) for these wind speed regimes.

Individual turbines displayed slight differences in the directional shear-affected wind speed regimes for a 0.225 deg m^{-1} threshold (not shown), but all turbines presented agreement in mean and median performance differences for 6.5 – 8 m s^{-1}. Turbine A exhibited significant differences in mean normalized power production (95% confidence) for 4.5 – 5 m s^{-1} and 5.5 – 8 m s^{-1} wind regimes, while median normalized performance also included 10 – 10.5 m s^{-1} and excluded 4.5 – 5 m s^{-1}. Turbine B displayed similar agreement among the affected wind regimes, as both mean and median normalized power had significant differences at the 5% level for 5.5 – 8 m s^{-1}, however the mean also included the 4 – 4.5 m s^{-1} regime and the median included near rated speeds (10 – 10.5 m s^{-1}). Matching mean and median normalized power differences in Turbine C occurred between 4.5 – 5.5 m s^{-1} and 6 – 8 m s^{-1}. Finally, Turbine D displayed the lowest agreement as both mean and median normalized power were distinct at the 5% level for 5.5 – 6 m s^{-1} and 6.5 – 8 m s^{-1}; the mean also captured differences for 5 – 5.5 m s^{-1}, and the median for 4 – 5 m s^{-1} and 10 – 10.5 m s^{-1}. Inner and outer turbines (Turbines B and C, and Turbines A and D, respectively) showed no distinction in the affected wind speed regimes or underperformance values. However, Turbine A and B displayed high agreement in their affected wind speed regimes and underperformance values ($\rho = 0.9986, p = 0.001$). Resemblance between Turbines C and D in their respective underperformance for wind speeds between 5.5 – 6 m s^{-1} and 6.5 – 8 m s^{-1} was much lower ($\rho = 0.7575, p = 0.2425$).

Wind Energ. Sci. Discuss., https://doi.org/10.5194/wes-2019-22
Manuscript under review for journal Wind Energ. Sci.
Discussion started: 14 May 2019

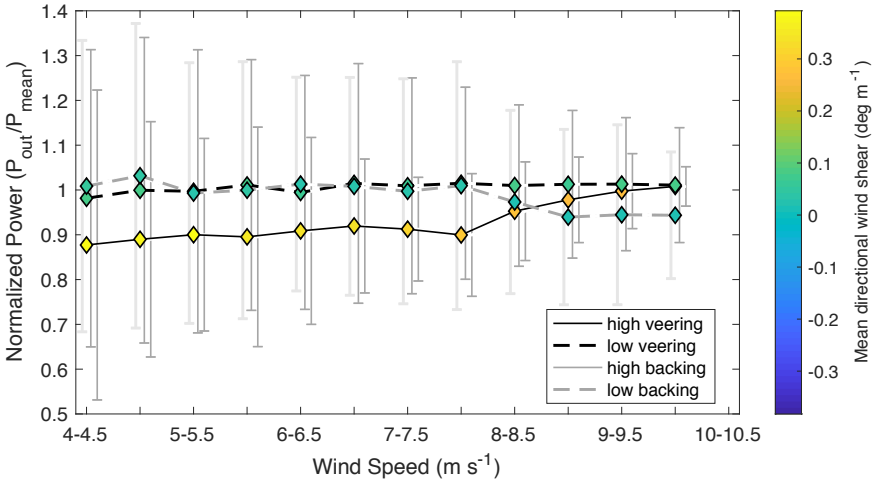

Figure 12. Mean normalized power production for high and low wind veering and backing scenarios defined using a threshold of ±0.225 deg m^{-1}. Error bars represent 1 standard deviation. Only 0.5 m s^{-1} wind speed bins with more than 30 data points are plotted.

Observed turbine underperformance was found to be determined by high veering scenarios. Figure 12 shows combined-turbine normalized performance segregating for high- and low- veering and backing scenarios using a threshold of ±0.225 deg m^{-1}. Differences between high-veering cases and high-backing cases cannot be compared as observed high backing atmospheric conditions reported less than 30 10-min events for all analyzed 0.5 m s^{-1} wind speed bins and turbines. Nonetheless, we can compare high veering to low veering and low backing. Combined-turbine mean normalized performance was significantly (99% confidence) reduced during high wind veering scenarios for 4 – 8 m s^{-1} wind speeds compared to low veering and backing cases. Mean normalized power did not evidence significant differences (1% significance) between low wind veering and backing for this wind speed range.

Wind Energ. Sci. Discuss., https://doi.org/10.5194/wes-2019-22
Manuscript under review for journal Wind Energ. Sci.
Discussion started: 14 May 2019

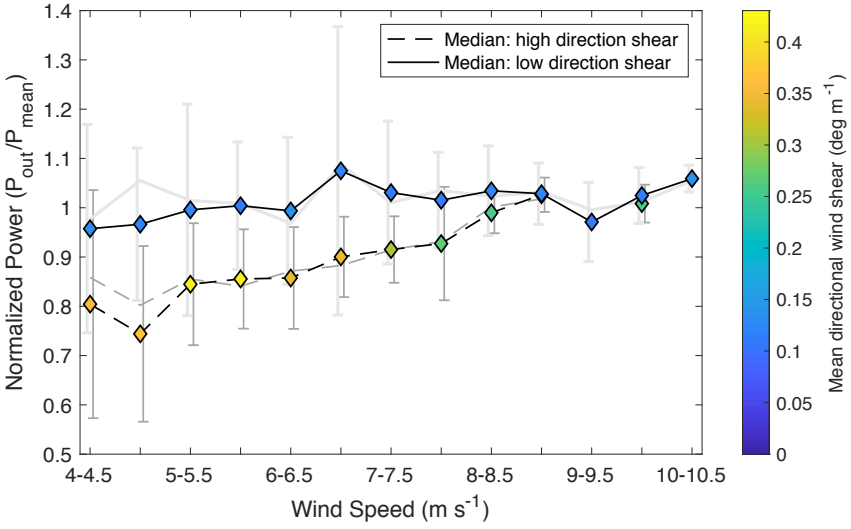

Figure 13. Normalized power production for high and low directional wind shear scenarios defined using a threshold of 0.225 deg m^{-1} from 0530 to 0900 local time. Black lines correspond to median values and grey ones to mean values. Error bars represent 1 absolute deviation from the median. Only 0.5 m s^{-1} wind speed bins with more than 30 data points are plotted.

Power variability can exert significant impact during morning hours, when power demand tends to increase. Throughout all power production periods, from 0530 to 0900 local time, the averaged directional wind shear was 0.2064 deg m^{-1} for wind speeds between 4 and 10.5 m s^{-1}. Combined-turbines mean and median normalized power production were significantly (99% confidence for the means and 95% confidence for the medians) affected by HDWS (threshold of 0.225 deg m^{-1}) for 4.5 – 8 m s^{-1} wind speed regimes (Figure 13). Mean underperformance was larger than 15% and median normalized power reductions were slightly larger than 12% for high directional shear compared to low directional shear scenarios.

5 Discussion and Conclusions

Directional wind shear at the test site showed more veering cases than backing cases (Figure 6a), as would be expected from the balance between Coriolis, pressure gradient, and frictional forces in the atmospheric boundary layer (Holton and Hakim, 2013). Furthermore, the largest directional shear values occurred between 40 m and 60 m above the surface (Figure 6b), as would also be expected given that turbulent fluxes increase near the surface, causing larger wind vector rotation near the ground.

Directional shear depends on time of day (Figure 7) as well as wind speed (Figure 8). The observed diurnal pattern is consistent with daily radiative flux cycles. The advent of short-wave radiation from the sun at dawn drives convective air plumes from surface heating causing the largest rate of directional shear decrease. Rising air parcels transport air with similar zonal and meridional speed components across the rotor layer, decreasing directional wind shear. As the sun keeps shining through the day, the convective atmosphere is strengthened, and directional wind shear tends to stabilize. Once the

short-wave radiative flux ceases at dusk, atmospheric stratification develops, evident from increasing directional shear values. A previous study in this same site found stable stratification to develop at 1900 local time and strong veering to develop after the evening transition (Lee and Lundquist, 2017). Median nighttime directional shear was at least 1.8 times larger than daytime, consistent with decoupled surface and residual layers within the atmospheric boundary layer. The upper portion of the ABL starts decoupling from that close to the ground as convective turbulent fluxes no longer maintain homogeneity in the atmosphere. Vanderwende et al. (2015) found strong, persistent low-level jets during nighttime at this site, which tend to further increase directional shear compared to daytime cases. Changes in wind direction with height tend to increase throughout the night, suggesting that the rotor-layer never equilibrated during nighttime.

As directional shear varied through different wind speeds, its effect on turbine performance also varied. Directional wind shear exerted a larger impact on power production near cut-in wind speeds than near rated wind speeds (Figure 10). This effect amplifies as the threshold between HDWS cases and LDWS cases increases, confirming that higher directional shear has detrimental effects on performance. However, statistically significant effects on turbine power output consistently occurred only in the mid-region of the partial load regime. All examined HDWS thresholds above 0.15 deg m^{-1} exposed significant combined-turbine mean normalized power reductions for wind speeds between 5 and 8 m s^{-1}. Rareshide et al. (2009) found minor effects of wind backing on turbine performance, however these were only depicted for hub-height wind speeds of 8 m s^{-1}. Walter et al. (2009) show a similar tendency for simulations performed for 8 and 10 m s^{-1} wind speeds. Here, we considered the effects of directional shear at lower wind speed regimes and found that more detrimental effects take place below 8 m s^{-1}.

In distinguishing the effects of HDWS from LDWS using a threshold of 0.225 deg m^{-1}, high directional shear reduced power output by nearly 10% compared to low directional shear scenarios for wind speeds below 8 m s^{-1}. Mean and median statistical significance tests were unanimous when considering combined-turbine performance on wind speed ranges between and 5 – 8 m s^{-1}. These findings contrast results found by Bardal et al. (2015), where directional shear larger than 5º over a 100 m rotor layer (0.05 deg m^{-1}) is found to have its major effects between 9 and 11 m s^{-1}. However, their test site presented land/sea interfaces and most of the analyzed winds came from offshore and so their data likely includes the development of an internal boundary layer due to roughness changes. Also, as is evidenced in Figure 9, our data presented low directional wind shear for near rated speeds: less than 4.5% of wind speeds above 8 m s^{-1} presented directional shear above 0.225 deg m^{-1}. In addition, directional shear in this site proves to be a major factor affecting turbine performance as 11% of partial load power production took place during HDWS atmospheric conditions between 4 and 8 m s^{-1} wind speeds.

Wind backing, as opposed to wind veering, was not found to affect performance in this dataset. High wind veering dominated over backing and revealed significant mean combined-turbine normalized power reductions for 4 – 8 m s^{-1} wind speeds. Rareshide et al. (2009) only found positive directional shear to reduce performance for 0.2 wind shear exponents and veering above 0.25 deg m^{-1}, whereas backing always resulted in underperformance. However, as was noted above, their results only considered 8 m s^{-1} wind speeds. Turbine performance simulations using a linear wind speed and direction change across the rotor layer by Walter et al. (2009), however, depicted slight underperformance (around 2 – 4% power change) for

wind veering greater than 0.2 deg m^{-1} and wind shear exponents near 0.3. Previous studies near this site (Walton et al., 2014) have shown power-law exponents around 0.4 to be dominant during nighttime in June, July and August; thus, the significantly larger effects found in this study may also be driven by a simultaneous large wind speed shear.

Focusing on a period of rapidly increasing electricity demand (0530 to 0900 local time) exposed the fact that directional shear's detrimental effects preferentially occur during this time. Mean normalized power reductions were larger for this time period (~15%) compared to whole-day results (~9%) for wind speeds between 4.5 and 8 m s^{-1}. Mean directional wind shear in this wind speed regime was 0.1886 deg m^{-1}, and 34.76% of observations presented directional shear larger than 0.225 deg m^{-1}. Not only did wind direction shear occur often during this high-demand period of the day, but it also undermined power production at this time.

The substantial power reductions and number of cases affected by the change of wind direction with height in this wind farm make directional wind shear effects meaningful when considering atmospheric conditions that affect wind turbines' power production. Though this study was not able to resolve conflicting results on the effects of atmospheric stability on turbine performance, it highlights the importance of considering the effects of wind direction shear. We recommend that the magnitude and incidence of large changes of wind direction with height (>0.1 deg m^{-1}) should be studied at the sites of the conflicting studies to confirm the existence of this phenomenon. Further, since directional wind shear is highly correlated with speed shear, a higher understanding of the effects of direction shear can be obtained by separating the effects of each of these conditions, but would likely require a much larger dataset. The effects of direction shear when distinguishing between the different atmospheric stability regimes should also be examined. Analyzing the effects of directional shear on stable, neutral and convective atmospheric conditions could shed light into conflicting results and help determine if site-specific factors govern these diverging findings.

The direction change of the wind vector with height not only affects inflow conditions for wind turbines, but also alters how wakes evolve downwind. Wakes evolving under directional wind shear conditions skew to form an ellipsoid as they are advected downstream (Abkar et al., 2016; Aitken et al., 2014; Bhaganagar and Debnath, 2014; Bodini et al., 2017; Churchfield and Sirnivas, 2018; Englberger and Dörnbrack, 2018). Churchfield and Sirnivas (2018) performed aeroelastic simulations for turbines displaced laterally compared to an upstream turbine, finding an asymmetrical power variation explained by the mean flow asymmetry across the rotor disk caused by a skewed wake. These simulations evidenced an increase in power production when wind veering was present versus a non-direction-shear condition for certain turbine locations. Fleming et al. (2019) proved this power gain by employing a successful approach to taking advantage of wakes in wind farms (wake steering), evidencing approximately 13% increase in energy on a downstream turbine. On their study, Churchfield and Sirnivas (2018) also found an asymmetrical load-behavior variation for turbines displaced laterally compared to an upstream turbine. The impacts on wake recovery, and hence power generation, and the modification of mechanical loads (Sathe et al., 2013) consequently make directional wind shear meaningful for engineering wake models and wind farm layout and operation.

Further work regarding directional wind shear in offshore locations should also be pursued. A preliminary wind resource assessment on the coast of Massachusetts by Bodini et al. (2019) evidenced large changes in wind direction with height. Average values of 0.1 deg m^{-1} for summertime, and 0.05 deg m^{-1} for wintertime (Bodini et al., 2019) are near the threshold at which we found significant power reductions. Further, they also found the summer to have low turbulence dissipation rates, thus long-propagating skewed wakes may impact power production and loads on downwind turbines.

Acknowledgements

The CWEX project was supported by the National Science Foundation under the State of Iowa EPSCoR grant 1101284. The role of the University of Colorado Boulder in CWEX-13 was supported by the National Renewable Energy Laboratory. The authors thank NextEra Energy for providing the wind turbine power data. This work was authored [in part] by the National Renewable Energy Laboratory, operated by Alliance for Sustainable Energy, LLC, for the U.S. Department of Energy (DOE) under Contract No. DE-AC36-08GO28308. Funding provided by the U.S. Department of Energy Office of Energy Efficiency and Renewable Energy Wind Energy Technologies Office. The views expressed in the article do not necessarily represent the views of the DOE or the U.S. Government. The U.S. Government retains and the publisher, by accepting the 5 article for publication, acknowledges that the U.S. Government retains a nonexclusive, paid-up, irrevocable, worldwide license to publish or reproduce the published form of this work, or allow others to do so, for U.S. Government purposes.

References

Abkar, M., Sharifi, A. and Porté-Agel, F.: Wake flow in a wind farm during a diurnal cycle, Journal of Turbulence, 17(4), 420–441, doi:10.1080/14685248.2015.1127379, 2016.

Aitken, M. L., Kosović, B., Mirocha, J. D. and Lundquist, J. K.: Large eddy simulation of wind turbine wake dynamics in the stable boundary layer using the Weather Research and Forecasting Model, Journal of Renewable and Sustainable Energy, 6(3), 033137, doi:10.1063/1.4885111, 2014.

Bardal, L. M., Sætran, L. R. and Wangsness, E.: Performance Test of a 3MW Wind Turbine – Effects of Shear and Turbulence, Energy Procedia, 80, 83–91, doi:10.1016/j.egypro.2015.11.410, 2015.

van den Berg, G. P.: Wind turbine power and sound in relation to atmospheric stability, Wind Energy, 11(2), 151–169, doi:10.1002/we.240, 2008.

Bhaganagar, K. and Debnath, M.: Implications of Stably Stratified Atmospheric Boundary Layer Turbulence on the Near-Wake Structure of Wind Turbines, Energies, 7(9), 5740–5763, doi:10.3390/en7095740, 2014.

Blackadar, A. K.: Boundary Layer Wind Maxima and Their Significance for the Growth of Nocturnal Inversions, Bulletin of the American Meteorological Society, 38(5), 283–290, 1957.

Bodini, N., Zardi, D. and Lundquist, J. K.: Three-dimensional structure of wind turbine wakes as measured by scanning lidar, Atmospheric Measurement Techniques, 10(8), 2881–2896, doi:10.5194/amt-10-2881-2017, 2017.

Bodini, N., Lundquist, J. K. and Kirincich, A.: US East Coast Lidar Measurements Show Offshore Wind Turbines Will Encounter Very Low Atmospheric Turbulence, Geophysical Research Letters, doi:10.1029/2019GL082636, 2019.

Burton, T., Sharpe, D., Jenkins, N. and Bossanyi, E.: Wind energy: handbook, J. Wiley, Chichester ; New York., 2001.

Churchfield, M. and Sirnivas, S.: On the Effects of Wind Turbine Wake Skew Caused by Wind Veer: Preprint, National Renewable Energy Laboratory, Golden, CO., 2018.

Englberger, A. and Dörnbrack, A.: Impact of the Diurnal Cycle of the Atmospheric Boundary Layer on Wind-Turbine Wakes: A Numerical Modelling Study, Boundary-Layer Meteorology, 166(3), 423–448, doi:10.1007/s10546-017-0309-3, 2018.

Fleming, P., King, J., Dykes, K., Simley, E., Roadman, J., Scholbrock, A., Murphy, P., Lundquist, J. K., Moriarty, P., Fleming, K., van Dam, J., Bay, C., Mudafort, R., Lopez, H., Skopek, J., Scott, M., Ryan, B., Guernsey, C. and Brake, D.: Initial Results From a Field Campaign of Wake Steering Applied at a Commercial Wind Farm: Part 1, Wind Energy Science Discussions, 1–22, doi:10.5194/wes-2019-5, 2019.

General Electric: GE Energy 1.5MW Wind Turbine., 2009.

Holton, J. R. and Hakim, G. J.: An introduction to dynamic meteorology, Fifth edition., Academic Press, Amsterdam., 2013.

International Electrochemical Comission: Power performance measurements of electricity producing wind turbines, International Electrochemical Comission, Geneva, Switzerland., 2005.

Kaiser, K., Langreder, W., Hohlen, H. and Højstrup, J.: Turbulence Correction for Power Curves, in Wind Energy, edited by J. Peinke, P. Schaumann, and S. Barth, pp. 159–162, Springer Berlin Heidelberg, Berlin, Heidelberg., 2007.

Lee, J. C. Y. and Lundquist, J. K.: Observing and Simulating Wind-Turbine Wakes During the Evening Transition, Boundary-Layer Meteorology, 164(3), 449–474, doi:10.1007/s10546-017-0257-y, 2017.

Lundquist, J. K., Takle, E. S., Boquet, M., Kosovic, B., Rhodes, M. E., Rajewski, D., Doorenbos, R., Irvin, S., Aitken, M. L., Friedrich, K., Quelet, P. T., Rana, J., Martin, C. St., Vanderwende, B. and Worsnop, R.: Lidar observations of interacting wind turbine wakes in an onshore wind farm, EWEA meeting proceedings, 10–13, 2014.

Lundquist, J. K., Churchfield, M. J., Lee, S. and Clifton, A.: Quantifying error of lidar and sodar Doppler beam swinging measurements of wind turbine wakes using computational fluid dynamics, Atmospheric Measurement Techniques, 8(2), 907–920, doi:10.5194/amt-8-907-2015, 2015.

Muñoz-Esparza, D., Lundquist, J. K., Sauer, J. A., Kosović, B. and Linn, R. R.: Coupled mesoscale-LES modeling of a diurnal cycle during the CWEX-13 field campaign: From weather to boundary-layer eddies: COUPLED MESOSCALE-LES OF A DIURNAL CYCLE, Journal of Advances in Modeling Earth Systems, 9(3), 1572–1594, doi:10.1002/2017MS000960, 2017.

National Oceanic and Atmospheric Administration: NOAA Sunrise/Sunset Calculator. [online] Available from: https://www.esrl.noaa.gov/gmd/grad/solcalc/calcdetails.html, 2019.

Rajewski, D. A., Takle, E. S., Lundquist, J. K., Oncley, S., Prueger, J. H., Horst, T. W., Rhodes, M. E., Pfeiffer, R., Hatfield, J. L., Spoth, K. K. and Doorenbos, R. K.: Crop Wind Energy Experiment (CWEX): Observations of Surface-Layer, Boundary Layer, and Mesoscale Interactions with a Wind Farm, Bulletin of the American Meteorological Society, 94(5), 655–672, doi:10.1175/BAMS-D-11-00240.1, 2013.

Rajewski, D. A., Takle, E. S., Lundquist, J. K., Prueger, J. H., Pfeiffer, R. L., Hatfield, J. L., Spoth, K. K. and Doorenbos, R. K.: Changes in fluxes of heat, H2O, and CO2 caused by a large wind farm, Agricultural and Forest Meteorology, 194, 175–187, doi:10.1016/j.agrformet.2014.03.023, 2014.

Rajewski, D. A., Takle, E. S., Prueger, J. H. and Doorenbos, R. K.: Toward understanding the physical link between turbines and microclimate impacts from in situ measurements in a large wind farm: MICROCLIMATE WITH TURBINES ON VERSUS OFF, Journal of Geophysical Research: Atmospheres, 121(22), 13,392-13,414, doi:10.1002/2016JD025297, 2016.

Rareshide, E., Tindal, A., Johnson, C., Graves, A., Simpson, E., Bleeg, J., Harris, T. and Schoborg, D.: Effects of Complex Wind Regimes on Turbine Performance, 2009.

Rhodes, M. E. and Lundquist, J. K.: The Effect of Wind-Turbine Wakes on Summertime US Midwest Atmospheric Wind Profiles as Observed with Ground-Based Doppler Lidar, Boundary-Layer Meteorology, 149(1), 85–103, doi:10.1007/s10546-013-9834-x, 2013.

Sathe, A., Mann, J., Barlas, T., Bierbooms, W. A. A. M. and van Bussel, G. J. W.: Influence of atmospheric stability on wind turbine loads: Atmospheric stability and loads, Wind Energy, 16(7), 1013–1032, doi:10.1002/we.1528, 2013.

St. Martin, C. M., Lundquist, J. K., Clifton, A., Poulos, G. S. and Schreck, S. J.: Wind turbine power production and annual energy production depend on atmospheric stability and turbulence, Wind Energy Science, 1(2), 221–236, doi:10.5194/wes-1-221-2016, 2016.

Stull, R. B.: An introduction to boundary layer meteorology, Kluwer Academic Publishers, Dodrecht., 1988.

Sumner, J. and Masson, C.: Influence of Atmospheric Stability on Wind Turbine Power Performance Curves, Journal of Solar Energy Engineering, 128(4), 531, doi:10.1115/1.2347714, 2006.

U.S. Energy Information Administration: U.S. Electric System Operating Data: Regional electricity demand (Midwest), U.S. Energy Information Administration. [online] Available from: https://www.eia.gov/realtime_grid/#/data/graphs?end=20180708T00&start=20180701T00&dataTypes=k&bas=00000000000g&regions=04, 2019.

Van de Wiel, B. J. H., Moene, A. F., Steeneveld, G. J., Baas, P., Bosveld, F. C. and Holtslag, A. A. M.: A Conceptual View on Inertial Oscillations and Nocturnal Low-Level Jets, Journal of the Atmospheric Sciences, 67(8), 2679–2689, doi:10.1175/2010JAS3289.1, 2010.

Vanderwende, B. and Lundquist, J. K.: Could Crop Height Affect the Wind Resource at Agriculturally Productive Wind Farm Sites?, Boundary-Layer Meteorology, 158(3), 409–428, doi:10.1007/s10546-015-0102-0, 2016.

Vanderwende, B. J. and Lundquist, J. K.: The modification of wind turbine performance by statistically distinct atmospheric regimes, Environmental Research Letters, 7(3), 034035, doi:10.1088/1748-9326/7/3/034035, 2012.

Vanderwende, B. J., Lundquist, J. K., Rhodes, M. E., Takle, E. S. and Irvin, S. L.: Observing and Simulating the Summertime Low-Level Jet in Central Iowa, Monthly Weather Review, 143(6), 2319–2336, doi:10.1175/MWR-D-14-00325.1, 2015.

Wagner, R., Courtney, M., Larsen, T. J. and Schmidt Paulsen, U.: Simulation of shear and turbulence impact on wind turbine performance, Danmarks Tekniske Universitet, Denmark. [online] Available from: http://orbit.dtu.dk/files/4550246/ris-r-1722.pdf, 2010.

Walpole, R. E., Ed.: Probability & statistics for engineers & scientists, 8th ed., Pearson Prentice Hall, Upper Saddle River, NJ., 2007.

Walter, K., Weiss, C. C., Swift, A. H. P., Chapman, J. and Kelley, N. D.: Speed and Direction Shear in the Stable Nocturnal Boundary Layer, Journal of Solar Energy Engineering, 131(1), 011013, doi:10.1115/1.3035818, 2009.

Walton, R. A., Takle, E. S. and Gallus, W. A.: Characteristics of 50–200-m Winds and Temperatures Derived from an Iowa Tall-Tower Network, Journal of Applied Meteorology and Climatology, 53(10), 2387–2393, doi:10.1175/JAMC-D-13-0340.1, 2014.

Wharton, S. and Lundquist, J. K.: Assessing atmospheric stability and its impacts on rotor-disk wind characteristics at an onshore wind farm: Atmospheric stability on rotor-disk wind characteristics, Wind Energy, 15(4), 525–546, doi:10.1002/we.483, 2012a.

Wind Energ. Sci. Discuss., https://doi.org/10.5194/wes-2019-22
Manuscript under review for journal Wind Energ. Sci.
Discussion started: 14 May 2019

Wharton, S. and Lundquist, J. K.: Atmospheric stability affects wind turbine power collection, Environmental Research Letters, 7(1), 014005, doi:10.1088/1748-9326/7/1/014005, 2012b.